

# Synthesis of $[\text{RuX}(\text{CO})\{\eta^2\text{-C,N-C}_6\text{H}_4\text{C(H)=NC}_6\text{H}_4\text{-4-NO}_2\}(\text{PPh}_3)_2]$ ( $\text{X} = \text{F, Cl, Br, I}$ ): Evidence of Non-Conventional Ru–X Hydrogen Bonds Leading to Octahedral Coordination at the Halide Atom

Kevin R. Flower,<sup>\*[a]</sup> Robin G. Pritchard,<sup>[a]</sup> and John E. Warren<sup>[a]</sup>

**Keywords:** Ruthenium / Cyclometallated ligands / Charge transfer / Hydrogen bonds / Pi interactions

Treatment of  $[\text{RuCl}(\text{CO})\{\eta^2\text{-C,N-C}_6\text{H}_4\text{C(H)=NC}_6\text{H}_4\text{-4-NO}_2\}(\text{PPh}_3)_2]$  (**4-Cl**) with  $\text{Ag}[\text{BF}_4]$  in acetone/ $\text{CH}_2\text{Cl}_2$  gives the cationic complex  $[\text{Ru}\{\text{O}=\text{C}(\text{CH}_3)_2\}(\text{CO})\{\eta^2\text{-C,N-C}_6\text{H}_4\text{C(H)=NC}_6\text{H}_4\text{-4-NO}_2\}(\text{PPh}_3)_2][\text{BF}_4]$  (not isolated), which then reacts with  $\text{NaX}$  ( $\text{X} = \text{F, Br, I}$ ) to afford the new compounds  $[\text{RuX}(\text{CO})\{\eta^2\text{-C,N-C}_6\text{H}_4\text{C(H)=NC}_6\text{H}_4\text{-4-NO}_2\}(\text{PPh}_3)_2]$  ( $\text{X} = \text{F, Br, I}$ ) (**4-F**, **4-Br**, and **4-I**). All of the new compounds have been characterised by elemental analysis (C, H, and N),  $^1\text{H}$ ,  $^{13}\text{C}\{^1\text{H}\}$ ,  $^{31}\text{P}\{^1\text{H}\}$  NMR spectroscopy and IR spectroscopy. The IR data support the hypothesis that the fluoride ligand is the strongest halogen  $\pi$ -donor to the metal centre. In addition, the compounds **4-Br**·1.5 $\text{CHCl}_3$ , **4-Cl**·1.5 $\text{CHCl}_3$ , **4-F**·2 $\text{CDCl}_3$ ,

and **4-I**·1.5 $\text{CHCl}_3$  have been characterised by single-crystal X-ray diffraction studies; all show  $\text{Ru-X}\cdots\text{HCCl}_3$  interactions with the Ru–F interaction being the strongest. In addition, there is evidence for the presence of competing  $\text{RuX}\cdots\text{ClCHCl}_2$  ( $\text{X} = \text{Cl, Br}$ ) interactions in compounds **4-Br** and **4-Cl**; these appear to be charge transfer in nature. The generality of these interactions has been probed using searches of the Cambridge Crystallographic Database and the data obtained suggests that these interactions have some, but limited, precedence.

(© Wiley-VCH Verlag GmbH & Co. KGaA, 69451 Weinheim, Germany, 2003)

## Introduction

There was an initial reluctance to accept the possibility of the hydrogen bond, from its first mention in 1902,<sup>[1]</sup> based upon the chemical dogma that hydrogen has a valence of one.<sup>[2]</sup> The hydrogen bond first reached the mainstream in Pauling's book *The Nature of the Chemical Bond*<sup>[3]</sup> in which the electrostatic nature of the interaction was emphasised. In 1960 Pimentel and McClellan modified the definition of a hydrogen bond to: "A hydrogen bond is said to exist when (1) there is evidence of a bond, and (2) there is evidence that this bond sterically involves a hydrogen atom involved in a bond to another atom."<sup>[4]</sup> Conventionally, hydrogen bonds involved hydrogen atom interactions with electronegative elements and donor groups such as N–H, O–H, halogen–H, with conventional acceptors based upon the same atoms in different hybridisation states.<sup>[5]</sup> Non-conventional interactions recognise the potential of, for example, C–H, P–H, M–H systems, to act as donors and  $\pi$ -systems (aryl, acetylenic) and C–F, for example, to act as acceptors. These and other secondary intermolecular interactions that influence solid-state structures are currently of much interest, with hydrogen bonding of particular note, due to its importance in biological systems,<sup>[6]</sup> non-covalent synthesis,<sup>[7]</sup> crystal engineering,<sup>[8]</sup> ca-

talysis,<sup>[9,10]</sup> and anion recognition,<sup>[11]</sup> to name but a few. A recent review of hydrogen bonding in the solid state has also recently appeared.<sup>[12]</sup> In addition to the hydrogen bond it has been recognised<sup>[13]</sup> that the halogens, Cl, Br, and I, may also interact with electronegative atoms via weak secondary interactions. The nature of these interactions has been subject to much debate. It has been shown that covalently bound halogen atoms do not occupy spherical volumes in space but are ellipsoidal due to the anisotropic distribution of electron density about their nucleus.<sup>[14,15]</sup> This leads to a non-uniform van der Waals radius that is shorter in the C–X bond direction. This so-called polar flattening has been used to explain why there are close intermolecular halogen $\cdots$ halogen contacts. Allen et al. have shown, however, that intermolecular contacts between the halogen (Cl, Br, and I) and the electronegative (O, N) atoms can exist,<sup>[16]</sup> and strong intermolecular halogen $\cdots$ halogen interactions have been reported, for example, for chlorine monofluoride.<sup>[17]</sup>

Based on methodology developed by Roper and Wright<sup>[18]</sup> we recently reported<sup>[19,20]</sup> the preparation of some cycloruthenated azobenzene-containing complexes of the type  $[\text{RuX}(\text{CE})(\eta^2\text{-C,N-C}_6\text{H}_4\text{N=NC}_6\text{H}_5)(\text{PPh}_3)_2]$  ( $\text{X} = \text{Cl, Br, I}$ ;  $\text{E} = \text{O, S}$ ) and subsequently extended the methodology to the preparation<sup>[21]</sup> of complexes of the type  $[\text{RuCl}(\text{CO})\{\eta^2\text{-C,N-C}_6\text{H}_4\text{C(H)=NC}_6\text{H}_4\text{-4-R}\}(\text{PPh}_3)_2]$  (**1-Cl**, **2-Cl**, **3-Cl**, **4-Cl**;  $\text{R} = \text{NMe}_2, \text{Me, I, NO}_2$ ) which contain cycloruthenated 2-(phenylimino)phenyl ligands (Figure 1). The structural and spectroscopic characteristics of these

<sup>[a]</sup> Department of Chemistry, UMIST,  
P. O. Box 88, Manchester M60 1QD, United Kingdom  
Fax: (internat.) + 44-161/200-4559  
E-mail: k.r.flower@umist.ac.uk

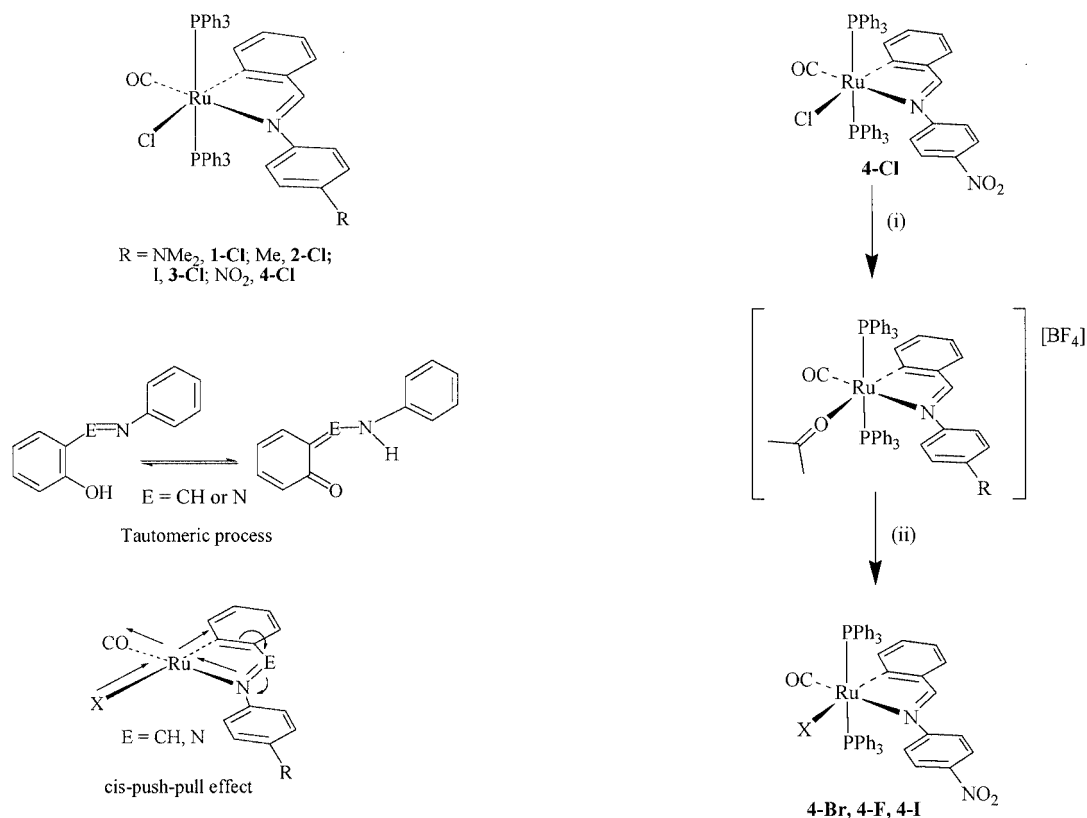


Figure 1. The analogy between the *cis*-push-pull effect and the tautomerisation in *ortho*-(hydroxy)azobenzenes and analogous Schiff bases

Scheme 1. (i)  $\text{Ag}[\text{BF}_4]$ ,  $\text{CH}_2\text{Cl}_2$ ,  $\text{OC}(\text{CH}_3)_2$ , 20 min; (ii)  $\text{NaX}$ ,  $\text{H}_2\text{O}$ ,  $\text{EtOH}$ , 1 h

Table 1. Physical, analytical and IR data for **4-Br**, **4-Cl**, **4-F**, and **4-I**

Compound <sup>[a][b]</sup>	Color	Yield (%)	C, H, N microanalysis: found (calcd.)			IR: $\nu(\text{CO})$ [ $\text{cm}^{-1}$ ]
<b>4-Br</b> $[\text{RuBr}(\text{CO})\{\eta^2\text{-}C,N\text{-C}_6\text{H}_4\text{C}(\text{H})=\text{NC}_6\text{H}_4\text{-4-NO}_2\}(\text{PPh}_3)_2] \cdot 1.5\text{CHCl}_3$	orange	93	54.7 (54.4)	3.9 (3.6)	2.9 (2.5)	1938
<b>4-Cl</b> $[\text{RuCl}(\text{CO})\{\eta^2\text{-}C,N\text{-C}_6\text{H}_4\text{C}(\text{H})=\text{NC}_6\text{H}_4\text{-4-NO}_2\}(\text{PPh}_3)_2] \cdot 1.5\text{CHCl}_3$	red	94	56.9 (56.6)	3.8 (3.7)	2.3 (2.6)	1929
<b>4-F</b> $[\text{RuF}(\text{CO})\{\eta^2\text{-}C,N\text{-C}_6\text{H}_4\text{C}(\text{H})=\text{NC}_6\text{H}_4\text{-4-NO}_2\}(\text{PPh}_3)_2] \cdot 2\text{CHCl}_3$	red	95	55.3 (55.0)	3.7 (3.6)	2.7 (2.5)	1923
<b>4-I</b> $[\text{RuI}(\text{CO})\{\eta^2\text{-}C,N\text{-C}_6\text{H}_4\text{C}(\text{H})=\text{NC}_6\text{H}_4\text{-4-NO}_2\}(\text{PPh}_3)_2] \cdot 1.5\text{CHCl}_3$	orange	96	52.4 (52.2)	3.7 (3.4)	2.8 (2.4)	1940

<sup>[a]</sup> Calculated values in parentheses. <sup>[b]</sup> Spectra recorded as Nujol mulls between KBr discs, all bands strong.

Table 2.  $^{31}\text{P}\{^1\text{H}\}$  NMR and  $^1\text{H}$  NMR data for compounds **4-Br**, **4-Cl**, **4-Br**, **4-F**, and **4-I**

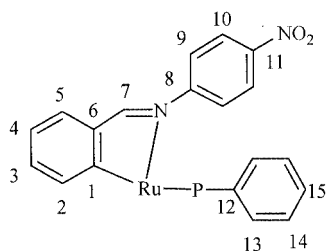
Compound <sup>[a]</sup>	$^{31}\text{P}$ ( $\delta$ )	$^1\text{H}$ ( $\delta$ )
<b>4-Br</b>	27.4	8.13 (t, $J_{\text{HP}} = 1.6$ , 1 H, CH=N), 7.56 (d, $J_{\text{H,H}} = 9.2$ , 2 H, aryl-H), 7.48–7.04 (m, 31 H, aryl-H), 6.56 (m, 2 H, aryl-H), 6.23 (d, $J_{\text{H,H}} = 9.2$ Hz, 2 H, aryl-H), 6.10 (t, $J_{\text{H,H}} = 7.0$ Hz, 1 H, aryl-H)
<b>4-Cl</b>	28.2	8.15 (t, $J_{\text{HP}} = 2.0$ , 1 H, CH=N), 7.59 (d, $J_{\text{H,H}} = 9.0$ , 2 H, aryl-H), 7.48–7.04 (m, 31 H, aryl-H), 6.60 (m, 2 H, aryl-H), 6.33 (d, $J_{\text{H,H}} = 9.0$ , 2 H, aryl-H), 6.12 (t, $J_{\text{H,H}} = 7.0$ Hz, 1 H, aryl-H)
<b>4-F</b>	26.9 (d, $J_{\text{PF}} = 15.3$ )	8.20 (t, $J_{\text{HP}} = 1.7$ , 1 H, CH=N), 7.69 (d, $J_{\text{H,H}} = 9.0$ , 2 H, aryl-H), 7.48–7.04 (m, 31 H, aryl-H), 6.93 (d, $J_{\text{H,H}} = 9.0$ Hz, 2 H, aryl-H), 6.74 (d, $J_{\text{H,H}} = 9.0$ , 1 H, aryl-H), 6.55 (t, $J_{\text{H,H}} = 7.0$ Hz, 1 H, aryl-H), 6.23 (t, $J_{\text{H,H}} = 7.4$ Hz, 1 H, aryl-H)
<b>4-I</b>	26.4	8.09 (t, $J_{\text{HP}} = 1.7$ , 1 H, CH=N), 7.55 (d, $J_{\text{H,H}} = 8.8$ , 2 H, aryl-H), 7.46–7.04 (m, 31 H, aryl-H), 6.59 (m, 2 H, aryl-H), 6.15 (t, $J_{\text{H,H}} = 7.6$ Hz, 1 H, aryl-H), 6.08 (d, $J_{\text{H,H}} = 8.8$ Hz, 2 H, aryl-H)

<sup>[a]</sup> Spectra recorded in  $\text{CDCl}_3$  at 293 K; coupling constants ( $J$ ) in Hz; s = singlet, d = doublet, t = triplet, m = multiplet.

Table 3.  $^{13}\text{C}\{^1\text{H}\}$  NMR data for **4-Br**, **4-Cl**, **4-F**, and **4-I**

Compound <sup>[a]</sup>	CO	C1	C2	C3	C4	C5	C6	C7	C8	C9	C10	C11	C12	C13	C14	C15
<b>4-Br</b>	206.9 (t, $J = 16.4$ )	191.9 (t, $J = 9.2$ )	141.1	130.7	120.3	131.6	142.4	175.2	154.8	125.4	122.3	145.1	133.5 (t, $J = 21.2$ )	134.1 (t, $J = 5.0$ )	127.6 (t, $J = 4.3$ )	129.3
<b>4-Cl</b>	206.7 (t, $J = 16.3$ )	191.9 (t, $J = 9.1$ )	141.1	130.8	120.1	131.3	142.3	174.9	154.9	125.2	122.5	145.0	133.3 (t, $J = 21.1$ )	134.0 (t, $J = 5.3$ )	127.6 (t, $J = 4.3$ )	129.3
<b>4-F</b>	206.4 (t, $J = 16.9$ )	192.9 (t, $J = 10.2$ ; t <sup>[b]</sup> , $J = 33.3$ )	141.1	130.4	119.8	131.2	142.7	172.1	154.6	124.4	123.2	144.9	132.8 (t, $J = 21.7$ )	133.6 (t, $J = 5.3$ )	127.7 (t, $J = 4.3$ )	129.4
<b>4-I</b>	207.6 (t, $J = 15.0$ )	192.7 (t, $J = 9.2$ )	141.1	130.7	120.5	131.9	142.8	175.6	154.7	125.8	122.2	145.1	133.7 (t, $J = 21.8$ )	134.3 (t, $J = 4.8$ )	127.5 (t, $J = 4.8$ )	129.3

<sup>[a]</sup> Spectra recorded in  $\text{CDCl}_3$  at 298 K; all resonances singlets unless otherwise stated; all  $J = J_{\text{PC}}$  [Hz] except: <sup>[b]</sup>  $J = J_{\text{FC}}$  [Hz].

Figure 2. Numbering scheme for  $^{13}\text{C}\{^1\text{H}\}$  NMR spectroscopic data

compounds afforded evidence for a *cis*-push-pull effect between the halide ligand and the CO ligand, which is moderated by the cyclometallated ligand. This effect was clearly

shown by comparison of the solid-state structures (X-ray) and  $^{13}\text{C}\{^1\text{H}\}$  NMR spectroscopic data obtained for **1-Cl**, **2-Cl**, **3-Cl**, and **4-Cl** with that obtained from previous studies concerned with the tautomeric process undergone by *ortho*-(hydroxy)azobenzene and [*ortho*-(hydroxy)phenylimino]-phenyl Schiff bases<sup>[22–24]</sup>. The effect was shown to be dependent on the *para* substituent of the phenylimino ring. We were then interested to see if the magnitude of the effect could be moderated by the  $\pi$ -donor strength of the halogen ligand. Herein we report that chloride/halogen exchange in **4-Cl** is readily facilitated by treatment with  $\text{Ag}^+$  followed by the reaction with  $\text{NaX}$  ( $\text{X} = \text{F}, \text{Br}, \text{I}$ ) and that the spectroscopic evidence shows that the fluoride ligand is the strongest  $\pi$ -donor. Furthermore, the solid-state structures

Table 4. Crystal data and data collection and refinement details for **4-Br**, **4-Cl**, **4-F** and **4-I**

	<b>4-Br</b>	<b>4-Cl</b>	<b>4-F</b>	<b>4-I</b>
Empirical formula	$\text{C}_{51.5}\text{H}_{40.5}\text{BrCl}_{4.5}\text{N}_2\text{O}_3\text{P}_2\text{Ru}$	$\text{C}_{51.5}\text{H}_{40.5}\text{Cl}_{5.5}\text{N}_2\text{O}_3\text{P}_2\text{Ru}$	$\text{C}_{52}\text{H}_{41}\text{Cl}_6\text{FN}_2\text{O}_3\text{P}_2\text{Ru}$	$\text{C}_{51.5}\text{H}_{40.5}\text{Cl}_{4.5}\text{IN}_2\text{O}_3\text{P}_2\text{Ru}$
Formula mass	1137.80	1093.34	1136.58	1184.79
$T$ [K]	150(2)	150(2)	150(2)	120(2)
Crystal size [mm]	$0.10 \times 0.10 \times 0.10$	$0.10 \times 0.10 \times 0.10$	$0.20 \times 0.10 \times 0.10$	$0.40 \times 0.18 \times 0.08$
$\lambda(\text{Mo-K}\alpha)$ [Å]	0.71073	0.71073	0.71073	0.71073
Crystal system	monoclinic	monoclinic	monoclinic	monoclinic
Space group	$P21/n$	$P21/n$	$P21/n$	$P21/n$
$a$ [Å]	10.9721(2)	11.0466(2)	12.03500(10)	10.9441(2)
$b$ [Å]	27.3926(6)	27.4903(5)	24.3670(3)	27.3627(6)
$c$ [Å]	16.0903(5)	15.8580(2)	18.0200(2)	16.3220(3)
$\beta$ [°]	90.8460(10)	90.00(1)	110.5450(10)	90.8640(10)
$V$ [Å <sup>3</sup> ]	4835.5(2)	4815.67(14)	5021.09(9)	4887.23(17)
$Z$	4	4	4	4
$d(\text{calcd.})$ [Mg/m <sup>3</sup> ]	1.563	1.508	1.504	1.610
$F(000)$	2292	2220	2304	2364
$2\theta$ range [°]	2.97–27.47	1.28–29.14	2.57–7.43	2.91–27.69
Total number of reflections collected	29592	38523	36273	35796
Independent reflections	10347	11221	11256	11000
$R(\text{int})$	0.0849	0.0809	0.0421	0.1057
Compl. to $\theta$ (%)	93.3	86.6	98.1	96.1
Data/restraints/parameter	10347/34/656	11221/29/648	11256/0/768	11000/12/748
GOF	1.021	1.024	1.031	1.033
$R1$ [ $I > 2\sigma(I)$ ]	0.0593	0.0531	0.0355	0.0524
$wR2$	0.1302	0.1134	0.0816	0.1345
$R1$ (all data)	0.1113	0.0872	0.0489	0.0767
$wR2$	0.1487	0.1274	0.0889	0.1472

of **4-Br**, **4-Cl**, **4-F**, and **4-I** display some interesting weak secondary interactions; in particular, the presence of  $\text{Ru}-\text{X}\cdots\text{HCCl}_3$  ( $\text{X} = \text{F}, \text{Cl}, \text{Br}, \text{I}$ ) and  $\text{Ru}-\text{X}\cdots\text{ClCCl}_2\text{H}$  ( $\text{X} = \text{Cl}, \text{Br}$ ) contacts, as well as hydrogen bonds to both the triphenylphosphane and cyclometallated ligands leading to essentially octahedrally coordinated halogen atoms.

## Results and Discussion

The compounds  $[\text{RuX}(\text{CO})\{\eta^2\text{-C}, \text{N-C}_6\text{H}_4\text{C}(\text{H})=\text{NC}_6\text{H}_4\text{-4-NO}_2\}(\text{PPh}_3)_2]$  ( $\text{X} = \text{Br}, \text{F}, \text{I}$ ) (**4-Br**, **4-F**, **4-I**) were prepared, in essentially quantitative yield, according to the

method illustrated in Scheme 1; i.e. treatment of **4-Cl** with a stoichiometric amount of  $\text{Ag}[\text{BF}_4]$  followed by, after filtration to remove  $\text{AgCl}$ , addition of a slight excess of  $\text{NaX}$  ( $\text{X} = \text{F}, \text{Br}, \text{I}$ ).

The new compounds **4-Br**, **4-F**, and **4-I** were all characterised by elemental analysis (C, H, N) and IR spectroscopy (Table 1),  $^1\text{H}$  and  $^{31}\text{P}\{^1\text{H}\}$  NMR spectroscopy (Table 2), and  $^{13}\text{C}\{^1\text{H}\}$  NMR spectroscopy (Table 3, see Figure 2 for the numbering scheme).

Compounds **4-Cl**, **4-Br**, **4-F**, **4-I** have also been characterised by single-crystal X-ray diffraction studies, see Table 4 for data collection and processing parameters, Table 5 for

Table 5. Selected bond lengths [ $\text{\AA}$ ] and angles [ $^\circ$ ] for **4-Br**, **4-Cl**, **4-F** and **4-I**

	<b>4-Br</b>	<b>4-Cl</b>	<b>4-F</b>	<b>4-I</b>
$\text{Ru}(1)-\text{X}$	2.6609(4)	2.5116(4)	2.1224(13)	2.8427(3)
$\text{Ru}(1)-\text{C}(1)$	2.050(3)	2.0527(13)	2.033(2)	2.059(3)
$\text{Ru}(1)-\text{N}(1)$	2.236(3)	2.2239(11)	2.2001(18)	2.241(2)
$\text{Ru}(1)-\text{C}(14)$	1.832(4)	1.8285(14)	1.823(2)	1.839(3)
$\text{C}(14)-\text{O}(1)$	1.156(4)	1.1554(17)	1.158(3)	1.143(4)
$\text{C}(7)-\text{N}(1)$	1.293(4)	1.3077(18)	1.295(3)	1.307(4)
$\text{C}(1)-\text{Ru}(1)-\text{X}$	169.90(10)	169.21(4)	166.42(7)	171.07(8)
$\text{C}(1)-\text{Ru}(1)-\text{N}(1)$	78.07(12)	78.31(5)	79.02(8)	77.97(10)
$\text{N}(1)-\text{Ru}(1)-\text{C}(14)$	167.05(12)	167.70(5)	171.58(9)	166.95(10)
$\text{N}(1)-\text{Ru}(1)-\text{X}$	92.54(7)	91.80(3)	87.40(6)	93.71(6)
$\text{C}(14)-\text{Ru}(1)-\text{X}$	100.18(10)	100.72(4)	100.09(8)	99.21(8)
$\text{C}(14)-\text{Ru}(1)-\text{C}(1)$	89.37(14)	89.39(6)	93.47(9)	89.24(11)
$\text{X}-\text{Ru}(1)-\text{P}(1)$	87.73(2)	86.816(12)	91.05(4)	89.462(18)
$\text{X}-\text{Ru}(1)-\text{P}(2)$	91.50(2)	91.452(12)	87.74(4)	90.529(18)
$\text{P}(1)-\text{Ru}(1)-\text{P}(2)$	173.57(3)	173.491(13)	174.59(2)	174.05(3)
$\text{Ru}(1)-\text{X}(1)-\text{H}(51)$	145.29(5)	145.22(6)	176.59(5)	142.4(4)
$\text{H}(9)-\text{X}(1)-\text{H}(40)$	149.90(5)	156.84(4)	169.03(4)	143.2(5)
$\text{H}(26)-\text{X}(1)-\text{H}(46)$	143.77(4)	146.39(7)	154.02(6)	137.9(4)

Table 6. Hydrogen bond data, distances [ $\text{\AA}$ ] and angles [ $^\circ$ ] for **4-Br**, **4-Cl**, **4-F**, **4-I**

Compound	Interaction	D-H	H $\cdots$ A	D $\cdots$ A	D-H $\cdots$ A
<b>4-Br</b>	$\text{C}(51)-\text{H}(51)-\text{Br}(1)$	1.00	3.02(3)	4.02(4)	173.1(3)
	$\text{C}(9)-\text{H}(9)-\text{Br}(1)$	0.95(3)	2.92(3)	3.385(5)	111.6(2)
	$\text{C}(26)-\text{H}(26)-\text{Br}(1)$	0.95(4)	2.81(4)	3.483(3)	128.7(5)
	$\text{C}(40)-\text{H}(40)-\text{Br}(1)$	0.95(4)	2.90(3)	3.536(3)	125.2(3)
	$\text{C}(46)-\text{H}(46)-\text{Br}(1)$	0.95(5)	2.76(3)	3.652(3)	157.3(4)
<b>4-Cl</b>	$\text{C}(51)-\text{H}(51)-\text{Cl}(\text{L}1)$	1.00	2.98(3)	3.963(2)	167.1(3)
	$\text{C}(9)-\text{H}(9)-\text{Cl}(\text{L}1)$	0.95(4)	2.79(3)	3.2935(14)	113.9(3)
	$\text{C}(26)-\text{H}(26)-\text{Cl}(\text{L}1)$	0.95(4)	2.68(3)	3.3617(15)	129.0(2)
	$\text{C}(40)-\text{H}(40)-\text{Cl}(\text{L}1)$	0.95(3)	2.79(3)	3.4534(14)	127.1(2)
	$\text{C}(46)-\text{H}(46)-\text{Cl}(\text{L}1)$	0.95(4)	2.71(4)	3.5934(15)	154.7(4)
<b>4-F</b>	$\text{C}(51)-\text{D}(51)-\text{F}(1)$	1.00(3)	1.81(3)	2.799(3)	172(3)
	$\text{C}(9)-\text{H}(9)-\text{F}(1)$	0.95(3)	2.32(3)	2.857(3)	115.1(19)
	$\text{C}(26)-\text{H}(26)-\text{F}(1)$	0.93(3)	2.24(3)	3.031(3)	143(2)
	$\text{C}(40)-\text{H}(40)-\text{F}(1)$	0.96(4)	2.23(3)	3.019(3)	139(2)
	$\text{C}(46)-\text{H}(46)-\text{F}(1)$	0.91(4)	2.59(3)	3.314(3)	141(9)
	$\text{C}(7)-\text{H}(7)-\text{O}(1)$	0.94(3)	2.63(3)	3.471(3)	169.3(4)
	$\text{C}(17)-\text{H}(17)-\text{O}(2)$	0.94(3)	2.581(3)	3.414(4)	149(2)
<b>4-I</b>	$\text{C}(3)-\text{H}(3)-\text{O}(3)$	0.93(3)	2.46(3)	3.327(3)	156(3)
	$\text{C}(51)-\text{H}(51)-\text{I}(1)$	1.05(2)	3.02(3)	4.053(3)	167.3(4)
	$\text{C}(9)-\text{H}(9)-\text{I}(1)$	1.00(2)	3.176(4)	3.553(2)	104(3)
	$\text{C}(26)-\text{H}(26)-\text{I}(1)$	1.02(3)	3.030(4)	3.60(3)	116.5(3)
	$\text{C}(40)-\text{H}(40)-\text{I}(1)$	1.00(3)	2.999(3)	3.647(2)	123.3(3)
	$\text{C}(46)-\text{H}(46)-\text{I}(1)$	0.95(3)	2.85(3)	3.737(2)	154.7(4)

selected bond lengths [ $\text{\AA}$ ], angles [ $^\circ$ ], Table 6 for hydrogen-bond data, Table 7 for halogen...halogen interaction data and Table 8 for selected torsion angles. ORTEP<sup>[25]</sup> represen-

Table 7. Halogen–halogen interaction, distances [ $\text{\AA}$ ] and angles [ $^\circ$ ] data for **4-Br** and **4-Cl**

Compound	$\text{C}(51)\text{--Cl}(1)$	$\text{Cl}(1)\cdots\text{X}$	$\text{C}(51)\cdots\text{X}$	$\text{C}(51)\text{--Cl}(1)\cdots\text{X}$
<b>4-Br</b>	1.665(5)	3.21(4)	4.966(5)	169.1(4)
<b>4-Cl</b>	1.710(4)	3.218(4)	4.916(4)	171.5(5)

Table 8. Selected torsion angles [ $^\circ$ ] for **4-Br**, **4-Cl**, **4-F**, **4-I**

Compound	$\text{Ru--P}(1)\text{--C}(21)\text{--C}(26)$	$\text{Ru--N}(1)\text{--C}(8)\text{--C}(9)$	$\text{Ru--P}(2)\text{--C}(39)\text{--C}(40)$	$\text{Ru--P}(2)\text{--C}(45)\text{--C}(46)$
<b>4-Br</b>	5.0(3)	−54.5(4)	0.9(3)	52.4(3)
<b>4-Cl</b>	6.21(14)	−52.87(18)	−1.94(14)	53.05(13)
<b>4-F</b>	13.4(2)	−41.7(3)	−16.7(2)	61.25(19)
<b>4-I</b>	1.5(3)	−56.6(4)	5.9(3)	53.0(3)

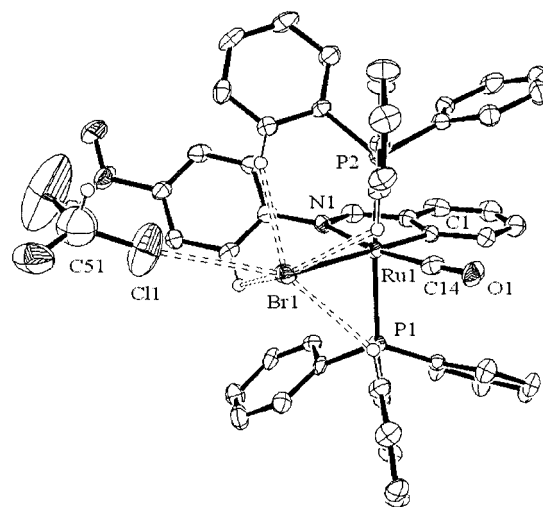
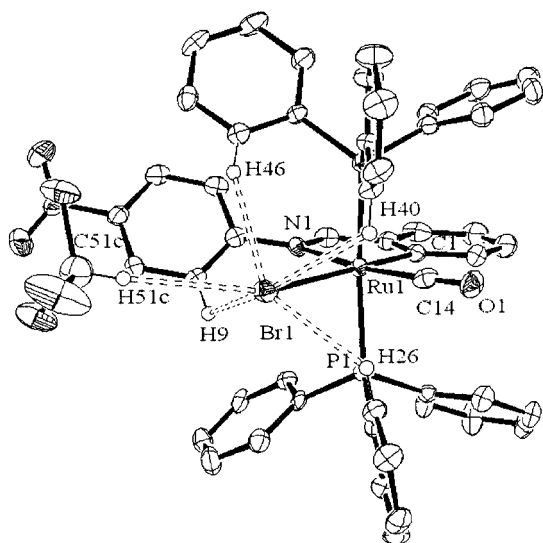


Figure 3. ORTEP representation of **4-Br** showing non-conventional interactions at the bromide ligand; thermal ellipsoids at 50%

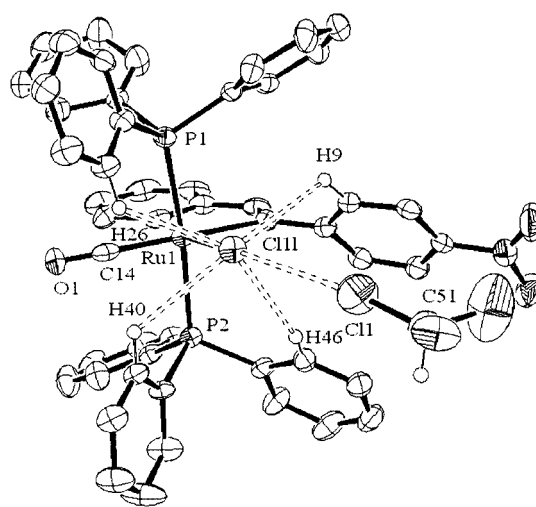
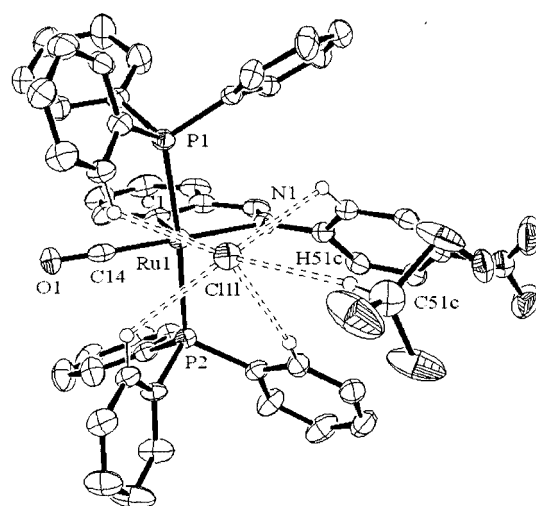


Figure 4. ORTEP representation of **4-Cl** showing non-conventional interactions at the chloride ligand; thermal ellipsoids at 50%



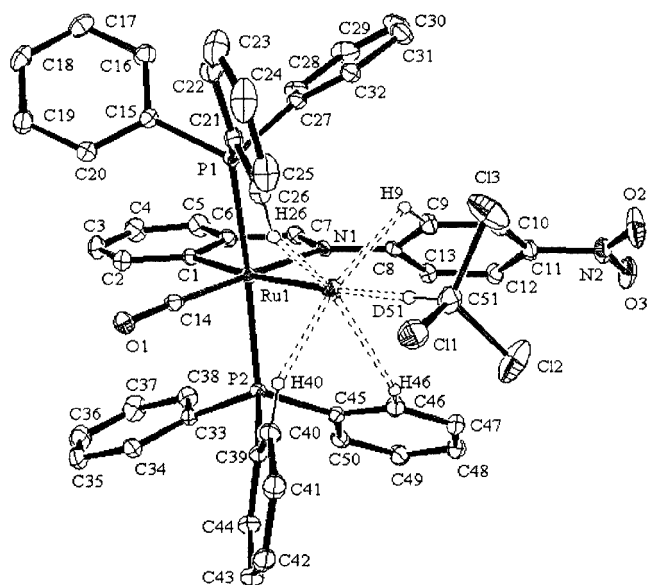


Figure 5. ORTEP representation of **4-F** showing non-conventional interactions at the fluoride ligand; thermal ellipsoids at 50%

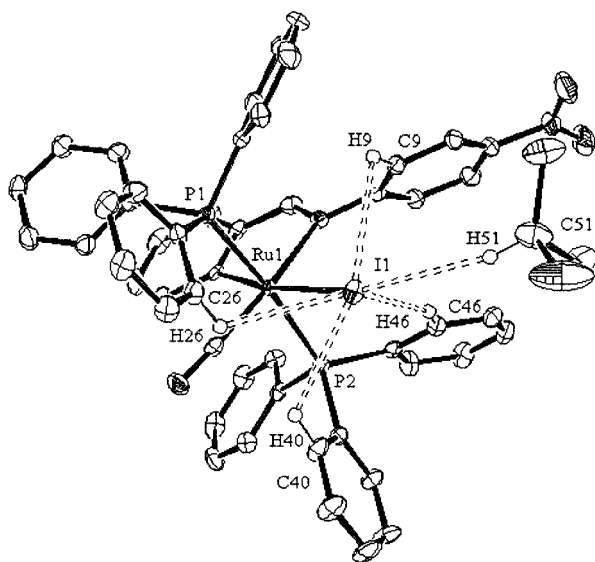


Figure 6. ORTEP representation of **4-I** showing non-conventional interactions at the iodide ligand; thermal ellipsoids at 50%

The IR spectra (Table 1) for **4-Cl**, **4-Br**, **4-F**, **4-I** all show a single strong  $\nu(\text{CO})$  band between 1923 (**4-F**) and 1940  $\text{cm}^{-1}$  (**4-I**). In a previous report<sup>[21]</sup> describing the synthesis of  $[\text{RuCl}(\text{CO})\{\eta^2\text{-C}_6\text{H}_4\text{C}(\text{H})=\text{NC}_6\text{H}_4\text{-4-R}\}(\text{PPh}_3)_2]$  ( $\text{R} = \text{NMe}_2, \text{Me}, \text{I}, \text{NO}_2$ ) **1-Cl**, **2-Cl**, **3-Cl**, **4-Cl** we were able to correlate the metallated carbon  $^{13}\text{C}\{^1\text{H}\}$  resonance with the Hammett  $\sigma^+$  parameter<sup>[26]</sup> which confirmed that the remote *para* substituent influences the *cis* push-pull effect (Figure 1); however, the trend in  $\nu(\text{CO})$  stretching frequencies was consistent with the  $^{13}\text{C}\{^1\text{H}\}$  NMR spectroscopic data, but not conclusive due to the narrow frequency separation across the series of 6  $\text{cm}^{-1}$ . For compounds **4-Cl**, **4-Br**, **4-F**, **4-I**, where the expected  $\pi$ -donor strength of the halide follows the trend  $\text{F} > \text{Cl} > \text{Br} > \text{I}$  with a con-

stant *para* substituent ( $\text{NO}_2$ ), the  $\nu(\text{CO})$  decreases across the series  $\text{I} > \text{Br} > \text{Cl} > \text{F}$ . This observation is consistent with the fluoride ligand being the strongest  $\pi$ -donor, Table 1 (note: the wavenumber separation across the whole series is 17  $\text{cm}^{-1}$ ). It should also be remembered that the orthogonal halide p-orbital will be involved in *cis*- $\pi$ -donation to the CO ligand, in this case mediated by a metal  $d_\pi$ -orbital, not the cyclometallated ligand.<sup>[27]</sup> It must therefore be a combination of both processes that accounts for the differences in the observed  $\nu(\text{CO})$  values observed for **4-Cl**, **4-Br**, **4-F**, **4-I**. Compelling evidence for this trend in  $\pi$ -donor strength for the halides ( $\text{F} > \text{Cl} > \text{Br} > \text{I}$ ) to transition metal centres has been noted previously.<sup>[28]</sup>

The compounds **4-Cl**, **4-Br**, **4-I** all show the expected singlet resonance in their  $^{31}\text{P}\{^1\text{H}\}$  NMR spectra Table 1, whereas for **4-F** a doublet is observed with  $J_{\text{P,F}} = 15.3 \text{ Hz}$ . The resonance position is barely perturbed on halogen exchange.

The  $^1\text{H}$  NMR spectroscopic data are consistent with the formulation of **4-Cl**, **4-Br**, **4-F**, **4-I**. All the compounds show a triplet resonance for the imine CH proton (coupling to the mutually *trans*-phosphane ligands). The presence of solvents of crystallisation is often seen in the  $^1\text{H}$  NMR spectra due to the propensity of these compounds to entrain solvent in the crystal lattice. For example, recrystallisation<sup>[21]</sup> of **4-Cl** from  $\text{CH}_2\text{Cl}_2$  and EtOH afforded **4-Cl**·1.5 $\text{CH}_2\text{Cl}_2$ , indeed the rapidity of recrystallisation process can affect the amount of solvent incorporated and microanalytical data need to be correlated with the NMR spectroscopic data. This is equally true for compounds **1-Cl**, **2-Cl** and **3-Cl**.<sup>[21]</sup>

The  $^{13}\text{C}\{^1\text{H}\}$  NMR spectra were assigned with the aid of DEPT-135 spectra substituent effects<sup>[29]</sup> and the data previously reported<sup>[21]</sup> for **1-Cl**, **2-Cl**, **3-Cl**, **4-Cl**, and are consistent with the formulation of **4-Br**, **4-Cl**, **4-F**, **4-I**.

#### The Solid-State Structures of **4-Br**, **4-Cl**, **4-F**, **4-I**

The presence of conventional N–H or O–H hydrogen bonds to high-valent metal fluoride complexes is well documented,<sup>[30]</sup> as is the presence of both conventional and non-conventional hydrogen bonds to organometallic complexes containing a fluoride ligand.<sup>[31]</sup> A search of the CDS<sup>[32]</sup> revealed only one other example<sup>[33]</sup> of a chloroform molecule hydrogen-bonding to a transition metal fluoride. In this case, to a fluoro-iron-porphyrin  $[\text{C}-\text{H}\cdots\text{F}, \text{C}-\text{H} 0.96(5); \text{H}\cdots\text{F} 2.11(5); \text{C}-\text{H}\cdots\text{F} 136(4)]$ . This interaction is considerably longer (17%) than that observed in **4-F** (Table 6). The shorter nature of the hydrogen bond interaction in **4-F** is presumably because the interaction, in this case, is with the radially less diffuse sp lone pair of the fluoride ligand. Work by others<sup>[34,35]</sup> on M–Cl systems, however, has shown a preference for the p-type lone pair to be more basic and interact with a hydrogen-bond donor (angular preference 100–110°).<sup>[35]</sup> This type of donor approach is ruled out in this system because of the steric bulk of the ancillary ligand set. Further analysis<sup>[36]</sup> of the crystallographic data revealed that four non-conventional intramolecular hydrogen bonds from the ancillary ligand phenyl ring hydrogen atoms H(9), H(26), H(40) and H(46) to the fluoride ligand

complete an essentially octahedral environment about the fluorine atom. In addition to these intramolecular hydrogen bonds the presence of three intermolecular hydrogen bonds was also observed: one to each of the carbonyl and nitro group oxygen atoms (Table 6, Figure 7).

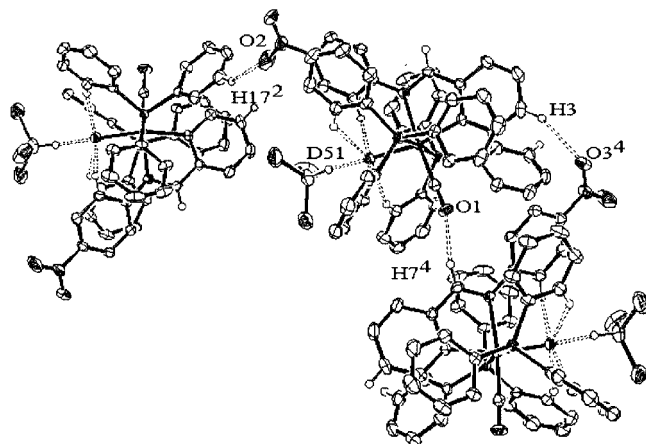


Figure 7. ORTEP representation of **4-F** showing both inter- and intramolecular hydrogen bonds; thermal ellipsoids at 50%

Since perusal of CDS<sup>[32]</sup> suggested that no complete series of  $\text{M-X}\cdots\text{HCCl}_3$  ( $\text{X} = \text{F}, \text{Cl}, \text{Br}, \text{I}$ ) hydrogen bond interactions had been reported to-date **4-Br**, **4-Cl**, **4-I** were recrystallised under conditions identical to those used to obtain the crystals of **4-F**. In each case crystals suitable for an X-ray diffraction study were obtained.

On solving the X-ray data for **4-Br**, **4-Cl**, **4-I** it was found that the three structures are isostructural, but different from **4-F**. The difference is essentially due to the incorporation of 2 mol-equiv. of  $\text{CDCl}_3$  of crystallisation into the lattice of the latter, compared to 1.5 into the former three. For **4-Br**, **4-Cl**, **4-I** one  $\text{CHCl}_3$  of crystallisation interacts with the  $\text{Ru-X}$  bond and a second (half occupancy) is located on a crystallographic inversion site; the latter will not be discussed.

For compound **4-I**, an  $\text{Ru-I}\cdots\text{HCCl}_3$  hydrogen bond is clearly present (Figure 6, Table 6); however, for compounds **4-Br** and **4-Cl** this is not explicitly the case. The  $\text{CHCl}_3$  solvent molecule located close to the  $\text{Ru-X}$  ( $\text{X} = \text{Cl}, \text{Br}$ ) moiety is disordered. When the disorder was modelled for **4-Cl** it was found that there were two principal orientations of the  $\text{CHCl}_3$  molecule and when this model was used (allowing for variable occupancy) to decipher the disorder observed in **4-Br** it was found that the disorder is identical, save that the relative occupancies of the orientations differ. Thus, in addition to the  $\text{Ru-X}\cdots\text{HCCl}_3$  hydrogen bond illustrated in Figures 3 and 4, an  $\text{Ru-X}\cdots\text{ClCCl}_2\text{H}$  ( $\text{X} = \text{Cl}, \text{Br}$ ) interaction, substantially less than the sum of the van der Waals radii,<sup>[37]</sup> was found to be present for both compounds (Figures 3 and 4, Table 7). The  $\text{Ru-X}\cdots\text{ClCCl}_2\text{H}$  ( $\text{X} = \text{Cl}, \text{Br}$ ) interaction is present for **4-Cl** 39% and for **4-Br** 76% of the time. Since the same disorder model is applicable to both cases it appears that certain orientations of the  $\text{CHCl}_3$  molecule are preferred and there must be some

explanation for this. The  $\text{Ru-X}\cdots\text{HCCl}_3$  interaction is perfectly understandable; however, the  $\text{Ru-X}\cdots\text{ClCHCl}_2$  is not immediately so. The proposed  $\text{Ru-X}\cdots\text{ClCCl}_2\text{H}$  interaction observed for compounds **4-Br** and **4-Cl** [ $\text{X} = \text{Br}$  169.1(4);  $\text{X} = \text{Cl}$  171.5(5) °] is “essentially linear” and one possible explanation would be that charge transfer ( $n \rightarrow \sigma^*$ ) from the  $\text{Ru-X}$  moiety to the  $\text{C-Cl}$  bond could be responsible for these interactions. Since this type of interaction seemed unusual to us a search of the CDS database was carried out to discover if there was any generality to such interactions in the solid state. The initial searches carried out were generic and considered the possibility of any transition metal halide interaction with a chloro-containing hydrocarbon within the sum of the van der Waals radii. The results of these searches were as follows: for the transition metal chlorides 226 hits, metal bromides 32 hits, and transition metal iodides 17 hits. These data are presented as scatter plots, Figures 8–10; there were no metal fluoride interactions. What is striking, however, is the number of hits and the mean of  $\text{X-Cl-C}$  ( $\text{X} = \text{Cl}, \text{Br}, \text{I}$ ) with angles of 155.1, 163.1 and 164.8°, respectively. It is important to note here that no restrictions were put on the searches, so both inter- and intramolecular contacts are represented in the plots. On further narrowing the search to just interactions between a chloroform molecule chlorine atom and a transition metal bound chlorine atom, 44 (Cl) and 5 (Br) hits, respectively, were obtained. Scatter plots of the data are presented as Figures 11 and 12. For the  $\text{TM-Cl}\cdots\text{ClCHCl}_2$  system the angular range is generally greater than 150°, with one exception KOMFIB, which has an interaction angle of 75°. The  $\text{Cl}\cdots\text{Cl}$  approach is only 3.9% less than the sum of the van der Waals radii and, due to the nonspherical nature of van der Waals radii, it is unlikely that this is a noteworthy contact and can be ignored.

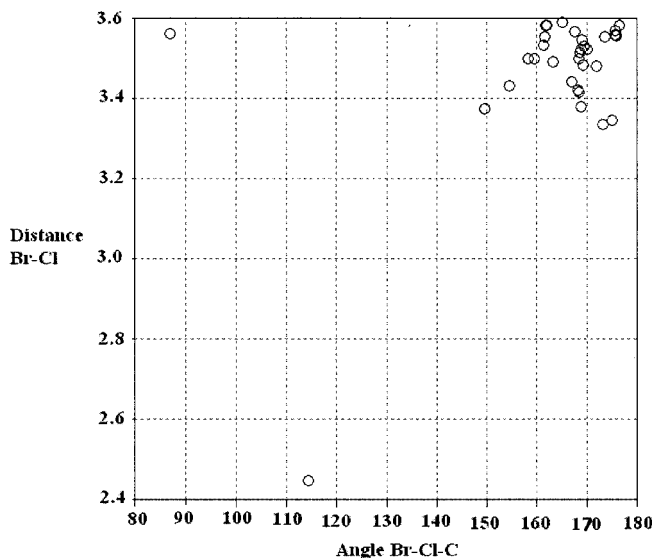


Figure 8. Scatter plot of  $\text{TMBR}\cdots\text{ClCR}$  distance [Å] versus  $\text{Cl}\cdots\text{ClCR}$  angle [°]

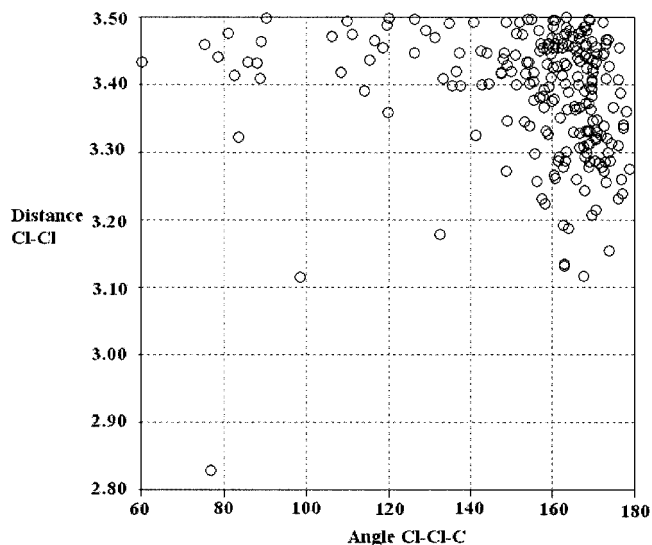


Figure 9. Scatter plot of  $\text{TMCl}\cdots\text{ClCR}$  distance [Å] versus  $\text{Cl}\cdots\text{ClCR}$  angle [°]

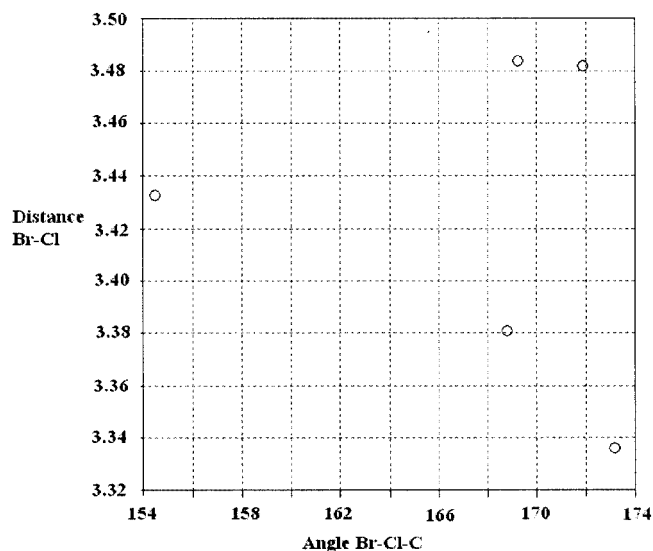


Figure 11. Scatter plot of  $\text{TMBR}\cdots\text{ClCHCl}_2$  distance [Å] versus  $\text{Cl}\cdots\text{ClCR}$  angle [°]

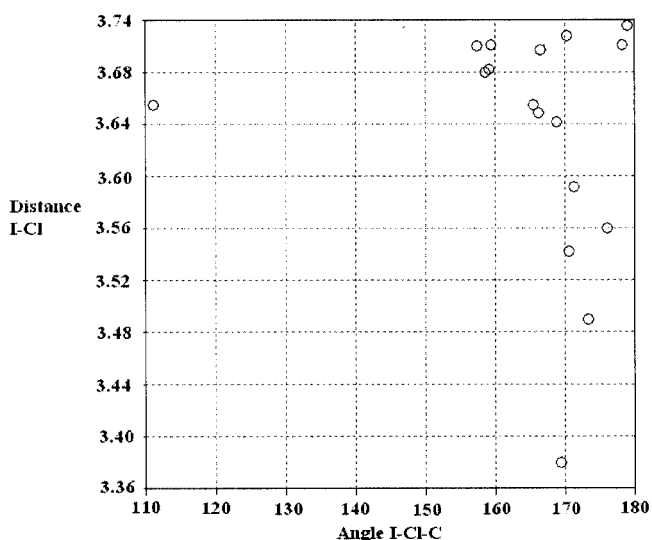


Figure 10. Scatter plot of  $\text{TMI}\cdots\text{ClCR}$  distance [Å] versus  $\text{Cl}\cdots\text{ClCR}$  angle [°]

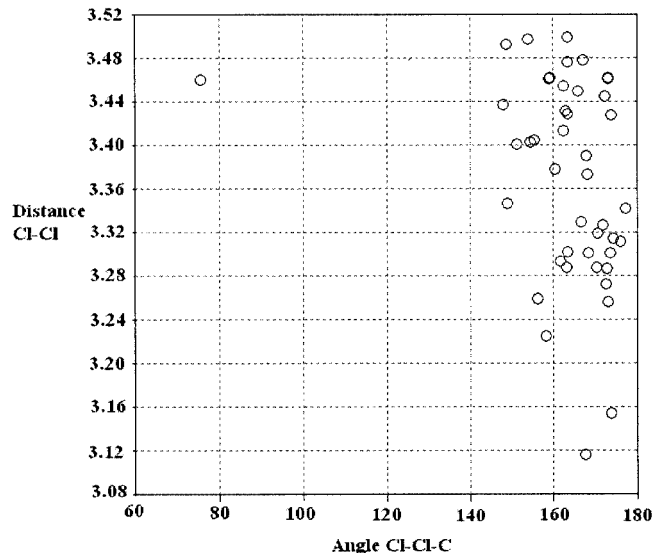


Figure 12. Scatter plot of  $\text{TMCl}\cdots\text{ClCHCl}_2$  distance [Å] versus  $\text{Cl}\cdots\text{ClCR}$  angle [°]

For the  $\text{TM}-\text{Br}\cdots\text{ClCHCl}_2$  system the angular range is greater than  $154^\circ$ , with four interactions greater than  $169^\circ$ . These plots show then that the chloroform interaction with the metal halide has mean  $\text{X}-\text{Cl}-\text{C}$  ( $\text{X} = \text{Br}, \text{Cl}$ ) angles of  $167.5$  and  $162.9^\circ$ , respectively, which are very close to linear. All the points are also comfortably within the sum of the van der Waals radii ( $3.75$  and  $3.60$  Å),<sup>[37]</sup> with the  $\text{Ru}-\text{X}\cdots\text{ClCCl}_2\text{H}$  ( $\text{X} = \text{Br}, \text{Cl}$ ) interaction observed for **4-Br** and **4-Cl** towards the shorter ends of the observed ranges (Figures 11 and 12). This would suggest that the  $\text{Ru}-\text{X}\cdots\text{Cl}$  ( $\text{X} = \text{Cl}, \text{Br}$ ) interactions observed in this system are real, supported at least by the presence of other comparable interactions present in the CDS, and qualitatively, at least, of comparable strength to the  $\text{Ru}-\text{X}\cdots\text{H}$  ( $\text{X} = \text{Br}, \text{Cl}$ ) interaction. The “linear” nature of these interactions is consistent

with the idea that that the interaction is charge-transfer in nature [ $\text{Ru}-\text{X}$  to the  $\text{C}-\text{Cl}$  bond ( $n \rightarrow \sigma^*$ )].

An alternative interpretation could be put forward based upon polar flattening. To invoke this argument a van der Waals radius approximately  $0.25$  Å less than the accepted value for each atom would be required if the interaction was to fall outside the sum of the van der Waals radii. When considered in conjunction with the following: compounds **4-F** and **4-I** form exclusively hydrogen-bonded interactions with the chloroform solvate; the strength of the hydrogen bond  $\text{Ru}-\text{X}\cdots\text{HCCl}_3$  would be expected to follow the trend  $\text{X} = \text{F} > \text{Cl} > \text{Br} > \text{I}$ ; the “disorder” is the same, save for relative occupancy, for **4-Br** and **4-Cl** (suggesting a preference for the chloroform’s orientation); it tends to make this approach less attractive in this case.



In addition to the electronic effects the increasingly bulky halide ligand exerts steric influences on the surrounding ligands, which manifests itself clearly in the orientation of the phenyl rings bearing the hydrogen atoms H(9), H(26), H(40) and H(46) that are involved in hydrogen bonding to the Ru–X halogen atoms. They all twist as expected to accommodate the increasing volume requirements of the halogen atom, or alternatively twist in to encapsulate the smaller halogen atom. Further, as a result of the increasing Ru–X bond length, not surprisingly, the octahedral coordination nature of the halogen atom becomes increasingly distorted on going from fluoride to iodide.

## Conclusion

We have readily effected halogen exchange in the compound  $[\text{RuCl}(\text{CO})\{\eta^2\text{-C}_6\text{H}_4\text{C}(\text{H})=\text{NC}_6\text{H}_4\text{-4-NO}_2\}(\text{PPh}_3)_2]$  to generate the family of compounds  $[\text{RuX}(\text{CO})\{\eta^2\text{-C}_6\text{H}_4\text{C}(\text{H})=\text{NC}_6\text{H}_4\text{-4-NO}_2\}(\text{PPh}_3)_2]$  ( $\text{X} = \text{F}, \text{Cl}, \text{Br}, \text{I}$ ) and shown that the fluoride ligand is the strongest  $\pi$ -donor. Further, on recrystallisation of the compounds **4-Br**, **4-Cl**, **4-F**, **4-I** from chloroform the Ru–X moiety forms a hydrogen bond to the chloroform of crystallisation and it is apparent that the strongest interaction, as expected, is to the fluorine atom. Unexpectedly, a competing  $\text{Ru}\cdots\text{ClCHCl}_2$  ( $\text{X} = \text{Cl}, \text{Br}$ ) interaction has been observed. In conjunction with data from a series of CDS searches, this interaction has been shown to have precedence and is possibly charge-transfer in nature. Further, intramolecular hydrogen bonds from phenyl ring hydrogen atoms of the  $\text{PPh}_3$  and the cyclometallated imine ligands to the halogen atom were observed in all of the compounds. This leads to essentially octahedral coordination about the halogen atom. The presence of these ancillary ligand phenyl–hydrogen interactions may well have implications for results obtained from theoretical calculations where, for example, the  $\text{PPh}_3$  ligand is simplified to  $\text{PH}_3$  as in a recent report detailing the mechanism of protonation of the  $\eta^2$ -allene ligand in  $[\text{ReCl}(\eta^2\text{-H}_2\text{C}=\text{C}=\text{CH}_2)(\text{dppe})_2]$  using the model compound  $[\text{ReCl}(\eta^2\text{-H}_2\text{C}=\text{C}=\text{CH}_2)(\text{PH}_3)_4]$ . In this study initial protonation was suggested to occur at the chloride ligand, but took no account of potentially competing hydrogen bond interactions from the dppe phenyl ring hydrogen atoms.<sup>[38]</sup>

## Experimental Section

**General Remarks:** All solvents, except alcohols, were dried by refluxing in the presence of an appropriate drying agent (toluene, Na;  $\text{CH}_2\text{Cl}_2$ ,  $\text{P}_4\text{O}_{10}$ ; hexane, NaK) and distilled prior to use.  $[\text{RuHCl}(\text{CO})(\text{PPh}_3)_3]$ <sup>[39]</sup> and  $[\text{RuCl}(\text{CO})\{\eta^2\text{-C}_6\text{H}_4\text{CH}=\text{NC}_6\text{H}_4\text{-4-NO}_2\}(\text{PPh}_3)_2]$ <sup>[21]</sup> were prepared according to literature procedures. All other chemicals were obtained from commercial sources and used as received except for  $\text{RuCl}_3$  which was loaned by Johnson Matthey. Infrared spectra were recorded as nujol mulls between KBr plates with a Nicolet 5PC spectrometer.  $^1\text{H}$  NMR (200.2 MHz) and  $^{31}\text{P}\{^1\text{H}\}$  NMR (81.3 MHz) were recorded with a

Bruker DPX200 spectrometer and  $^{13}\text{C}\{^1\text{H}\}$  NMR (100.55 MHz) were recorded with a Bruker DPX400 spectrometer.  $^1\text{H}$  and  $^{13}\text{C}\{^1\text{H}\}$  NMR spectra were referenced to  $\text{CHCl}_3$  ( $\delta = 7.26$  ppm) and  $\text{CHCl}_3$  ( $\delta = 77.0$  ppm) and  $^{31}\text{P}\{^1\text{H}\}$  NMR spectra were referenced externally to 85%  $\text{H}_3\text{PO}_4$  ( $\delta = 0.0$  ppm). Elemental analyses were performed by the Microanalytical Service, Department of Chemistry, UMIST; solvates of crystallisation were confirmed by repeated elemental analysis and confirmed by  $^1\text{H}$  NMR spectroscopy. The syntheses of all complexes were carried out under dinitrogen using standard Schlenk techniques. Workups were generally carried out in the open unless otherwise stated.

**$[\text{RuF}(\text{CO})\{\eta^2\text{-C}_6\text{H}_4\text{CH}=\text{NC}_6\text{H}_4\text{-4-NO}_2\}(\text{PPh}_3)_2]\cdot 2\text{CHCl}_3$  (**4-F**):**  $\text{Ag}[\text{BF}_4]$  (0.022 g, 0.11 mmol) was added to  $[\text{RuCl}(\text{CO})\{\eta^2\text{-C}_6\text{H}_4\text{CH}=\text{NC}_6\text{H}_4\text{-4-NO}_2\}(\text{PPh}_3)_2]$  (0.1 g, 0.11 mmol), dissolved in  $\text{CH}_2\text{Cl}_2/\text{acetone}$  (1:1, 10 mL) under a stream of dry  $\text{N}_2$ . After 20 min, the solution was filtered to remove  $\text{AgCl}$ , and  $\text{NaF}$  (0.05 g, 1.2 mmol), dissolved in  $\text{H}_2\text{O}$  (0.2 mL), was added followed by enough  $\text{EtOH}$  to generate a homogeneous solution. After 20 min, the organic solvent was removed under reduced pressure precipitating crude **4-F**. Collection by filtration and recrystallisation from  $\text{CHCl}_3$  afforded **4-F**· $2\text{CHCl}_3$  (0.118 g, 96%). Compounds **4-Br**, **4-Cl**, **4-I** were prepared in an analogous fashion; see Table 1 for physical and analytical data.

**X-ray Crystallographic Study:** All of the crystals were grown by the slow evaporation of chloroform from a 20-mg sample, initially dissolved in 0.5 mL of solvent in a lightly capped 5-mm NMR tube. All measurements were carried out with a Nonius Kappa CCD diffractometer using graphite-monochromated  $\text{Mo-K}\alpha$  radiation ( $\lambda = 0.71073$  Å) at 150 K for **4-Br**, **4-Cl**, **4-F** and 120 K for **4-I** at the National Crystallographic Service, University of Southampton, England. The structures were solved by direct methods using SHELXL-97<sup>[40]</sup> and subjected to full-matrix least-squares refinement on  $F^2$ . In **4-Br** and **4-Cl** the  $\text{CHCl}_3$  which interacts with the halogen ligand is disordered and was modelled using the same geometric restraints and with variable atomic site occupancies. Additionally for **4-Br**, **4-Cl** and **4-I**, the lattice  $\text{CHCl}_3$  is disordered about a crystallographic inversion point and was also modelled using geometric restraints, but in this case the atomic site occupancies were set to 0.5. In this case the disorder in **4-Br** and **4-Cl** was not the same. The crystallographic details are presented in Table 4. CCDC-172276, -172277, -172278, -1772279 (**4-F** to **4-I**) contain the supplementary crystallographic data for this paper. These data can be obtained free of charge at [www.ccdc.cam.ac.uk/conts/retrieving.html](http://www.ccdc.cam.ac.uk/conts/retrieving.html) [or from the Cambridge Crystallographic Data Centre, 12 Union Road, Cambridge CB2 1EZ, UK; Fax: (internat.) + 44-1223/336-033; E-mail: [deposit@ccdc.cam.ac.uk](mailto:deposit@ccdc.cam.ac.uk)].

## Acknowledgments

We thank the EPSRC National Crystallographic Service for data collections project number 01XR10, the EPSRC for the award of a postgraduate studentship to J. E. W. and Johnson Matthey for the kind loan of  $\text{RuCl}_3$ .

[1] A. Werner, *Justus Liebigs Ann. Chem.* **1902**, 322, 261–297.

[2] J. C. Speakman, *The Hydrogen Bond and Other Intermolecular Forces* (Monographs for Teachers, no. 27), The Chemical Society, London, **1975**, p. 8.

[3] L. Pauling, *The nature of the chemical bond*, Cornell University Press, Ithaca, New York, **1939**.

[4] G. C. Pimentel, A. L. McClellan, *The hydrogen bond*, W. H. Freeman, San Francisco, **1960**.

- [5] G. R. Desiraju, T. Steiner, *The Weak Hydrogen Bond in Structural Chemistry and Biology*, Oxford University Press, Oxford, **1999**.
- [6] G. A. Jeffrey, W. Saenger, *Hydrogen Bonding In biological Structures*, Springer-Verlag, Berlin, **1991**.
- [7] L. J. Prins, D. N. Reinhoudt, P. Timmerman, *Angew. Chem.* **2001**, *113*, 2446–2492; *Angew. Chem. Int. Ed.* **2001**, *40*, 2382.
- [8] G. R. Desiraju, *Crystal Engineering: the Design of Organic Solids*, Elsevier, Amsterdam, **1991**.
- [9] E. J. Corey, T. W. Lee, *Chem. Commun.* **2001**, 1321–1329.
- [10] M. Yamakawa, I. Yamada, R. Noyori, *Angew. Chem.* **2001**, *113*, 2900–2903; *Angew. Chem. Int. Ed.* **2001**, *40*, 2818–2821.
- [11] P. D. Beer, P. A. Gale, *Angew. Chem.* **2001**, *113*, 502–532; *Angew. Chem. Int. Ed.* **2001**, *40*, 486–516.
- [12] T. Steiner, *Angew. Chem.* **2002**, *114*, 58–80; *Angew. Chem. Int. Ed.* **2002**, *41*, 48–76.
- [13] N. Ramasubbu, R. Parthasarathy, P. Murry-Rust, *J. Am. Chem. Soc.* **1986**, *108*, 4308–4314.
- [14] S. C. Nyburg, W. Wong-Ng, *Proc. R. Soc. London A* **1979**, *367*, 29–45.
- [15] S. L. Price, A. J. Stone, J. Lucas, R. S. Rowland, A. E. Thornley, *J. Am. Chem. Soc.* **1994**, *116*, 4910–4918.
- [16] J. P. M. Lommerse, A. J. Stone, R. Taylor, F. H. Allen, *J. Am. Chem. Soc.* **1996**, *118*, 3108–3116.
- [17] R. Boese, A. D. Boese, D. Bläser, M. Yu, A. Ellerern, K. Sepelt, *Angew. Chem.* **1997**, *109*, 1538–1541; *Angew. Chem. Int. Ed. Engl.* **1997**, *36*, 1489 and refs therein.
- [18] W. R. Roper, L. J. Wright, *J. Organomet. Chem.* **1977**, *142*, C1–C6.
- [19] W. I. Cross, K. R. Flower, R. G. Pritchard, *J. Organomet. Chem.* **2000**, *601*, 164–171.
- [20] K. R. Flower, R. G. Pritchard, *J. Organomet. Chem.* **2001**, *620*, 60–68.
- [21] K. R. Flower, V. J. Howard, R. G. Pritchard, J. E. Warren, *Organometallics* **2002**, *21*, 1184–1189.
- [22] K. Venkataraman, *Synthetic Dyes*, vol. 1, Academic Press, New York, **1952**.
- [23] H. Zollinger, *Azo and Diazo Chemistry*, Wiley-Interscience, New York, **1961**.
- [24] L. Antonov, W. M. F. Fabian, D. Nedeltcheva, F. S. Kamounah, *J. Chem. Soc., Perkin Trans. 2* **2000**, 1173–1179.
- [25] C. K. Johnson, Report ORNL-5138, Oakridge National Laboratory, Tennessee, USA, **1976**.
- [26] J. March, *Advanced Organic Chemistry, Structure, Reaction, and Mechanisms*, 4th ed. Wiley Interscience, New York, **1992**, p. 28.
- [27] K. G. Caulton, *New J. Chem.* **1994**, *18*, 25–41.
- [28] K. Fagnou, M. Lautens, *Angew. Chem.* **2002**, *114*, 26–49; *Angew. Chem. Int. Ed.* **2002**, *41*, 26–47.
- [29] H. O. Kalinowski, S. Berger, S. Braun, *Carbon-13 NMR Spectroscopy*, Wiley-Interscience, New York, **1988**.
- [30] W. Massa, D. Babel, *Chem. Rev.* **1988**, *88*, 275–296.
- [31] T. G. Richmond, *Coord. Chem. Rev.* **1990**, *105*, 221–250.
- [32] F. H. Allen, J. E. Davies, O. J. Johnson, O. Kennard, C. F. Macrae, G. F. Mitchell, J. M. Smith, D. Watson, *J. Chem. Inf. Compt. Sci.* **1991**, *31*, 187–204.
- [33] S. C. Lee, R. H. Holm, *Inorg. Chem.* **1993**, *32*, 4745–4753.
- [34] G. P. A. Yap, A. L. Rheingold, P. Das, R. H. Crabtree, *Inorg. Chem.* **1995**, *34*, 3474–3476.
- [35] G. Aullón, D. Bellamy, L. Brammer, E. A. Bruton, A. G. Orpen, *Chem. Commun.* **1998**, 653–654.
- [36] A. L. Spek, *Platon (C)*, Utrecht University, Padualaan 8, 3584 CH, Utrecht, The Netherlands, **1900–2002**.
- [37] A. Bondi, *J. Phys. Chem.* **1964**, *68*, 441–451.
- [38] M. L. Kuznetsov, J. L. Pombeiro, A. I. Dement'ev, *J. Chem. Soc., Dalton Trans.* **2000**, 4413–4421.
- [39] N. Ahmad, J. J. Levison, S. D. Robinson, M. J. Uttley, *Inorg. Synth.* **1974**, *15*, 48–49.
- [40] G. M. Sheldrick *Programs for crystal structure analysis* (release 97-2), University of Göttingen, **1998**.

Received September 18, 2002